ACS OMEGA

Open Access

This article is licensed under CC-BY-NC-ND 4.0

http://pubs.acs.org/journal/acsodf

Article

Enhancing Aqueous Stability of Anionic Surfactants in High Salinity and Temperature Conditions with SiO_2 Nanoparticles

Mohammed H. Alyousef, Muhammad Shahzad Kamal,* Mobeen Murtaza, Syed Muhammad Shakil Hussain, Arshad Raza, Shirish Patil, and Mohamed Mahmoud

Cite This: *ACS Omega* 2024, 9, 49804−49815

Read Online

ACCESS | Metrics & More | Article Recommendations

ABSTRACT: In chemical-enhanced oil recovery (cEOR), surfactants are widely used but face significant stability challenges in high-salinity brine, where they often degrade or precipitate. Existing methods, such as adding cosurfactants, offer limited compatibility with anionic surfactants and raise economic concerns, creating a need for more robust solutions. This study introduces a novel approach to enhance the stability of anionic surfactants in extreme salinity conditions by incorporating silicon dioxide (SiO_2) nanoparticles (NPs). Our optimized formulation effectively prevents surfactant precipitation and NP aggregation, demonstrating stability in brine with salinity as high as 57,000 ppm and temperatures up to 70 °C, thus addressing the salt tolerance issues seen with conventional anionic surfactants like sodium dodecyl sulfate (SDS). To validate our formulation, we employed multiple experimental techniques, including turbidity, ζ-potential (ZP), and hydrodynamic diameter (HDD) measurements, which confirmed the efficacy of our approach. Results indicated that an optimal SiO_2 NP concentration (0.01 wt %) significantly enhanced SDS stability, with no observed aggregation or precipitation over 7 days. High absolute ZP values (>25 mV), a small HDD (∼37 nm), and a consistent turbidity profile underscored the stability and dispersion of the formulation. This nanoparticle-based method offers a cost-effective and sustainable solution for cEOR, providing enhanced surfactant stability and improved NP dispersibility under high-salinity and high-temperature conditions, representing a valuable advancement in chemical-enhanced oil recovery technology.

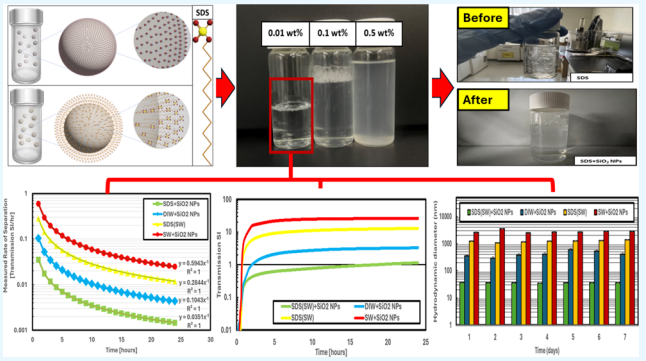

INTRODUCTION

Surfactants are highly valued in various industries for their ability to accumulate at interfaces and enhance the properties of solutions. Surfactants are essential in many applications, such as detergents, medical formulations, and anticorrosive treatments.[1,2] Surfactants are also crucial for cEOR applications in the petroleum industry.[3−7]

Anionic surfactants are notably the most widely used for cEOR applications.,[8] are vital in reducing IFT and altering reservoir rock wettability.[9] Despite their extensive use and study, challenges arise with anionic surfactants such as petroleum sulfonates, which exhibit excellent interfacial properties but suffer from poor salt resistance, leading to severe precipitation in high-salinity conditions.[10] This results from the poor aqueous stability of anionic surfactants in high-salinity solutions and limits the applicability of commercially available anionic surfactants for EOR applications.

Researchers have proposed the utilization of nonionic surfactants with anionic surfactants as a solution to address this issue. Nonionic surfactants serve as cosurfactants, enhancing the efficacy of anionic surfactants.[11] Particularly valuable in environments with high salinity, nonionic surfactants improve the aqueous stability of anionic surfactants.[12] However, several challenges exist in incorporating nonionic surfactants with anionic surfactants. Compatibility issues between nonionic and anionic surfactants are prevalent. Furthermore, the economic feasibility of integrating nonionic surfactants into anionic formulations may vary and may be influenced by factors such as the quantity and performance of the surfactants.

Another strategy involves utilizing nanoparticles (NPs), specifically silicon dioxide (SiO_2) NPs, to improve the performance of surfactants.[13,14] However, their stability and dispersibility under harsh conditions pose significant challenges to their use in EOR.[15] Traditionally, the stability of SiO_2 NPs is enhanced by incorporating surfactants, particularly anionic

Received: September 16, 2024
Revised: November 7, 2024
Accepted: November 21, 2024
Published: December 4, 2024

ACS Publications

© 2024 The Authors. Published by American Chemical Society

https://doi.org/10.1021/acsomega.4c08484
ACS Omega 2024, 9, 49804−49815

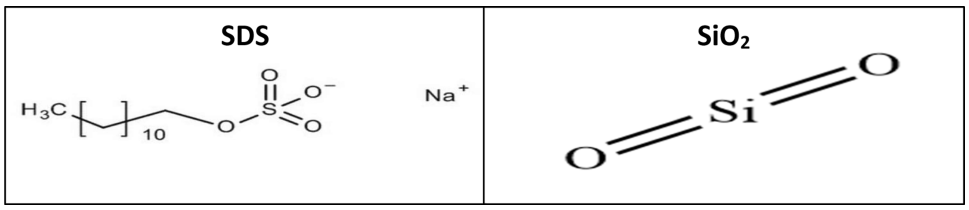

Figure 1. SDS and SiO_2 NP structures.

surfactants. These surfactants prevent NP aggregation by creating repulsive forces between surfactant molecules and NPs, thereby keeping them dispersed.[16,17]

SiO_2 NPs are commonly integrated with surfactants to create nanofluids, holding promise for future EOR projects and garnering significant attention in the scientific community.[18−20] Their ability to reduce IFT and facilitate spontaneous emulsion formation has been noted.[21,22] Additionally, the aqueous dispersion of SiO_2 NPs (<100 nm),[23] such as SiO_2 nanofluids, offers distinct advantages for EOR through wettability alteration in rock/fluid and fluid/fluid interactions.[24,25] Previous studies have observed substantial improvements in surfactant solutions and their efficacy in oil recovery processes with the introduction of NPs.[26,27]

However, previous investigations into SiO_2 nanofluids primarily focused on enhancing surfactant performance to recover more oil and did not address the enhancement of aqueous stability of anionic surfactants.[18,21,28] Also, some of these studies[16,29−33] have utilized deionized water (DIW) or low-salinity water as base fluids, which may not be practical in field applications, as seawater (SW) is usually used as a base fluid.

This is due to the significant challenges posed by commercially available anionic surfactants, which can precipitate severely in high-salinity base fluids. Furthermore, the aggregation and precipitation of NPs due to van der Waals forces in such fluids present additional challenges.[34,35] Other previous studies have primarily focused on utilizing SiO_2 NPs and surfactants at room temperature,[36,37] neglecting the effects of harsh temperature conditions that can lead to the degradation of surfactants or NPs. Thus, this study aims to consider all of the previous issues while utilizing SiO_2 NPs to enhance the aqueous stability of anionic surfactants under harsh conditions.

Our study introduces an innovative SiO_2 nanoparticle-based formulation that addresses anionic surfactant precipitation and SiO_2 nanoparticle aggregation under extreme salinity and temperature conditions. This innovative approach marks a significant advancement in the field of nanofluids as it is the first to leverage SiO_2 NPs to enhance the aqueous stability of anionic surfactants rather than solely focusing on improving surfactant performance for oil recovery. This breakthrough presents a cost-effective and sustainable solution to enhance oil recovery, particularly by utilizing SW salinity as a base fluid.

MATERIALS AND METHODS

In this study, sodium dodecyl sulfate (SDS), a commercially available anionic surfactant sourced from Sigma-Aldrich, was utilized, featuring a molecular weight of 288.38 g/mol, an HLB of 40, and was applied at a concentration of 0.25 wt %. Silicon dioxide (SiO_2) NPs from Sigma-Aldrich in nanopowder form were employed. Figure 1 illustrates the molecular structure of SDS alongside the nanoscale structure of SiO_2 NPs. These NPs exhibited a size range of 10−20 nm (BET), a molecular weight of 60.08 g/mol with 99.5% trace metals basis, and a 2.2−2.6 g/mL density at 25 °C, used at a 0.01 wt % concentration.

A surfactant solution was initially prepared by blending 0.5 wt % SDS in brine with total dissolved salts (TDS) of 57,000 ppm, which represents the Arabian Gulf seawater salt composition[38] (detailed in Table 1). This mixture was left overnight for enhanced dispersion. The SDS solution was diluted to 0.25 wt %, and a 0.01 wt % concentration of SiO_2 NPs was added while stirring. The final solution was stirred for an hour and then sonicated for 40 min at 80 kHz under room conditions.

Table 1. Arabian Gulf Seawater Salt Composition

salt	concentration (ppm)
NaCl	41,172
$CaCl_2{\cdot}2H_2O$	1802
$MgCl_2{\cdot}6H_2O$	8266
Na_2SO_4	6339
$NaHCO_3$	165
total dissolved salts (TDS)	57,745

This research employed diverse experimental techniques to evaluate the stability of formulations incorporating SiO_2 NPs with DIW, SW, and SDS. Also, SDS without NPs was prepared to compare its performance with our proposed formulation. Table 2 shows the formulations tested in this study and the concentration of each solution.

Table 2. Prepared Formulations in This Study

solution	SDS concentration (wt %)	SiO_2 concentration (wt %)	volume (mL)
SDS(SW) + SiO_2 NPs	0.25	0.01	25
SDS(SW)	0.25		25
SW + SiO_2 NPs		0.01	25
DIW + SiO_2 NPs		0.01	25

The stability assessment of the prepared formulations involved multiple methods, including visual tests conducted at both room temperature and 70 °C, turbidity tests at 70 °C for solutions containing SiO_2 NPs, ζ-potential (ZP) measurements, and hydrodynamic diameter (HDD) analysis to compare the stability between the proposed formulation with some of the previous formulations in the literature.

Initially, the investigation began with assessing the stability of solutions through visual observation. Two groups of formulations were made; one was exposed at room temperature, and the other was left in the oven at 70 °C. The formulations were left for 7 days and recorded with time to assess any observable changes.

Following initial visual assessments of stability over time, more robust techniques were employed to comprehensively investigate the solutions' stability. The second phase involved turbidity tests to assess particle settling by measuring sample

https://doi.org/10.1021/acsomega.4c08484
ACS Omega 2024, 9, 49804−49815

transmission. Turbidity tests are conducted by placing a sample containing NPs in a vial within a tower that continuously emits light onto the sample. The light transmission is measured to determine nanoparticle dispersion and stability.

Turbidity tests were conducted for an entire day on samples containing SiO_2 NPs at 70 °C to evaluate the stability of the proposed formulation compared to other formulations from the literature. These tests were performed using the *MultiScan MS 20* purchased from *DataPhysics* to ensure accuracy and reliability in assessing particle settling or aggregation.

The third phase involved conducting ZP measurements essential for assessing solution stability. These measurements were performed by filling a specialized vial with the liquid of interest and placing it inside the analyzer. The analyzer then applied an electric field, causing the particles to move in response to the interaction between their surface charges and the field. This interaction is used to determine the absolute value of the ZP.

ZP measurements offer valuable insights into the electrostatic repulsions between the prepared formulations, serving as a reliable indicator of solution stability, with higher absolute values of ZP indicating better stability.[39] The measurements were conducted over 7 days, with each test consisting of 100 runs and five repetitions. To minimize errors, an average curve was generated for each day.

Following the ZP measurements, HDD measurements were conducted to provide crucial information on particle aggregation. These measurements were performed using the same equipment as the ZP measurements. The HDD measurements determine particle size by measuring the random changes in the intensity of light scattered from a suspension or solution. Based on these changes, the machine calculates the average HDD of the solution. The procedure involved three runs per day, with five repetitions, and an average curve was derived each day for 7 days. ZP and HDD measurements were performed using the *LiteSizer DLS 100*, purchased from *Anton Paar*.

RESULTS AND DISCUSSION

Aqueous Stability. This section presents the findings from the visual tests of the proposed formulation, as outlined in Table 2. Multiple SiO_2 concentrations were tested before proceeding with other evaluations, as shown in Figure 2. It was determined

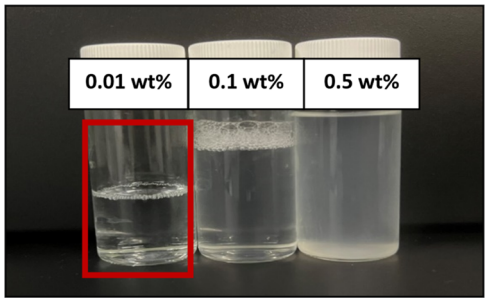

Figure 2. Different SiO_2 NP concentrations with SDS.

that a concentration of 0.01 wt % was optimal for dispersing SiO_2 NPs and preventing SDS precipitation. Lower SiO_2 NPs concentrations proved more effective and easier to disperse than higher concentrations, and they were utilized in many previous studies in the literature.[40−43] This is because, at lower concentrations, there are fewer particles, reducing the likelihood of collisions and aggregation. Conversely, higher concentrations of SiO_2 NPs increase the frequency of collisions, leading to greater aggregation, a phenomenon previously highlighted in the literature.[44]

SDS exhibits significant precipitation in high-salinity environments due to the abundance of ions, particularly positive ions like Na^+ and Ca^{2+}, which strongly induce precipitation.[45−47] These ions reduce the electrostatic repulsion between the negatively charged SDS molecules, increasing their aggregation and precipitation. Additionally, high salt concentrations increase the ionic strength of the solution, resulting in a "salting out" effect.[48,49] As illustrated in Figure 3, this effect decreases the solubility of SDS as the added ions compete with SDS molecules for water, making it difficult for SDS to remain dissolved, thus demonstrating SDS's intolerance to high salinities and poor aqueous stability. However, adding SiO_2 NPs markedly improves SDS stability and prevents precipitation. SiO_2 NPs enhance SDS aqueous stability in high-salinity environments through several mechanisms. The results obtained in this study suggest that they provide steric stabilization by creating a physical barrier around SDS molecules, preventing aggregation and precipitation. Additionally, they enhance electrostatic repulsion between SDS molecules, further reducing the likelihood of aggregation. This enhancement is demonstrated in Figure 4A when comparing SDS alone with SiO_2 nanofluid on a closer scale at a temperature of 25 °C.

It might be suggested that the observed precipitation behavior is due to the Krafft temperature, suggesting that the solution is below the Krafft point, which prevents micelle formation. The Krafft temperature or point is the minimum temperature required for surfactant molecules to form micelles; below this point, surfactants are less soluble and can crystallize or precipitate.[50,51] For SDS, the Krafft temperature in DIW is reported to be around 14 °C at a concentration of approximately 7000 ppm.[52] Notably, the Krafft temperature decreases as SDS concentration decreases. Above this temperature, micellar aggregates form, preventing crystallization. It has also been documented that increasing salt concentration raises the Krafft temperature of SDS and reduces its solubility in water.[53,54]

Since the experiments were conducted at 25 °C, it might seem that the Krafft temperature is responsible for the precipitation observed. However, there is no data on the Krafft temperature for the specific salinity and salt composition used in this study. While it is true that the Krafft temperature can increase with salt concentration, it is unlikely to reach 25 °C under the conditions tested. Previous studies have shown only a modest increase in Krafft temperature with higher salt concentrations.[52,54] Furthermore, the presence of precipitates at 70 °C, as illustrated in Figure 4B, is significantly above the Krafft point, suggesting that the Krafft temperature is not the primary factor. Instead, the high ionic strength of the solution—due to the presence of divalent ions in the complex SW solution—is likely the main cause of precipitation, as it weakens the electrostatic repulsion between SDS molecules. Thus, while the Krafft temperature may contribute to precipitation at 25 °C, it is not the primary mechanism.

Turbidity Test. Turbidity tests were conducted to verify the outcomes from visual observation regarding formulation stability. The turbidity scanning method detects agglomeration and sedimentation processes and quantifies nanoparticle stability levels.[55] The machine generates a transmission profile that indicates the sample's stability, whereas transmission relies on sample transparency.

https://doi.org/10.1021/acsomega.4c08484
ACS Omega 2024, 9, 49804−49815

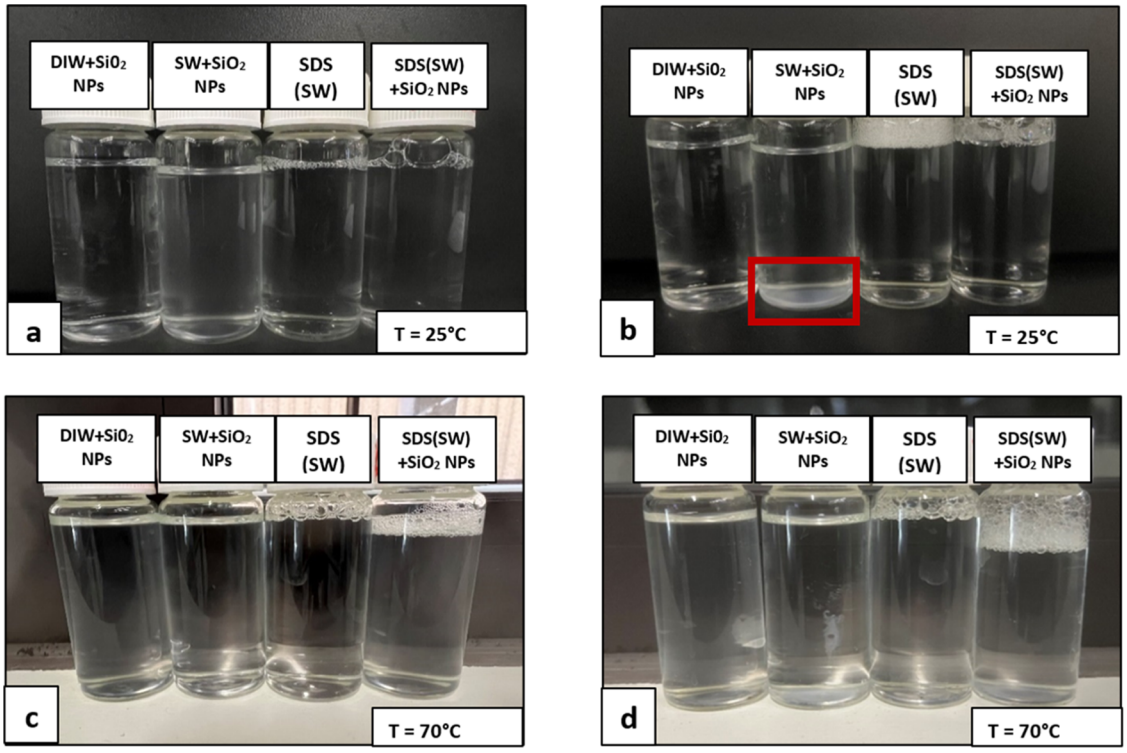

Figure 3. (a) Prepared formulations on day one at 25 °C, (b) prepared formulations on day seven at 25 °C, (c) prepared formulations on day one at 70 °C, and (d) Prepared formulations on day seven at 70 °C.

The transmission profile remains relatively consistent with dispersed and stable NPs. Conversely, it exhibits more significant variation in unstable NPs or molecules prone to aggregation and precipitation, marked by a significant difference between initial and final readings. This difference is due to increased transmission during precipitation events as aggregated particles settle, thereby improving sample transparency. Consequently, light can penetrate more effectively, leading to higher transmission compared to the initial state where NPs or molecules are uniformly dispersed and obstruct the passage of light.

The analysis of Figure 5 reveals notable trends in the transmission profiles of SiO_2 NPs with different base fluids and SDS in SW. In DIW, a slight increase in transmission is observed, indicating some settling of NPs, which allows light to pass through more easily, thereby increasing transmission. Conversely, SiO_2 NPs in SW exhibit significant instability, primarily due to interactions between the SiO_2 NPs and salt molecules. This instability is further exacerbated with SDS, which shows an even more unstable profile compared to SiO_2 nanofluid and SiO_2 in DIW. This is due to the prominent precipitation of SDS molecules caused by their instability in harsh salt conditions, as previously explained.

The substantial increase in transmission suggests nanoparticle aggregation and SDS precipitation, highlighting the limitations of using SiO_2 NPs or SDS alone in high-salinity base fluids. While previous illustrations in this paper indicated greater instability for SDS in SW, turbidity measurements taken on day one show less significant precipitation compared to what was observed on day seven. However, even on day one, our proposed formulation proved to be more stable. The formulation emerged as the most stable sample, displaying minimal changes in transmission. This minimal change indicates little settling over 24 h, underscoring the formulation's efficacy in maintaining nanoparticle dispersion and simultaneously preventing the aggregation and precipitation of SDS molecules. This highlights the successful enhancement of the aqueous stability of the anionic surfactant SDS through the novel use of SiO_2 NPs in high-salinity conditions.

Upon examining Figure 6, a clear stability hierarchy among the samples becomes evident. The illustration shows the Transmission Separation Index (TSI), which indicates how the solution's separation occurs over time and, consequently, its stability. The sample with the lowest TSI values over time is the most stable and shows the least signs of separation. The SiO_2 nanofluid exhibits the highest stability, characterized by its minimal TSI. NPs in DIW rank second in terms of TSI, followed by SDS in SW, which displays a less stable transmission profile than the first two. Notably, NPs in SW are the most unstable, highlighting the effectiveness of our proposed solution in simultaneously enhancing both the aqueous stability of SDS and the stability and dispersibility of SiO_2 NPs under challenging salinity conditions.

Additionally, Table 3 presents the separation rate equations derived from Figure 6 for each sample. The separation rate is inversely related to stability, meaning the lowest separation rate corresponds to the highest stability. Each measurement was conducted over a 24 h period, and the software generated equations to predict the separation rate for each sample. Figure 7 further illustrates the separation rate over time for the samples, along with the predicted separation rate equations generated by fitting the data. These predictions underscore the superior performance of our proposed formulation in maintaining nanoparticle dispersion and preventing aggregation and precipitation in high-salinity conditions.

As depicted in Figure 7, the separation rate of each formulation was determined using the equations provided in Table 3. The initial separation rates for SDS in SW, SiO_2 NPs in

https://doi.org/10.1021/acsomega.4c08484
ACS Omega 2024, 9, 49804−49815

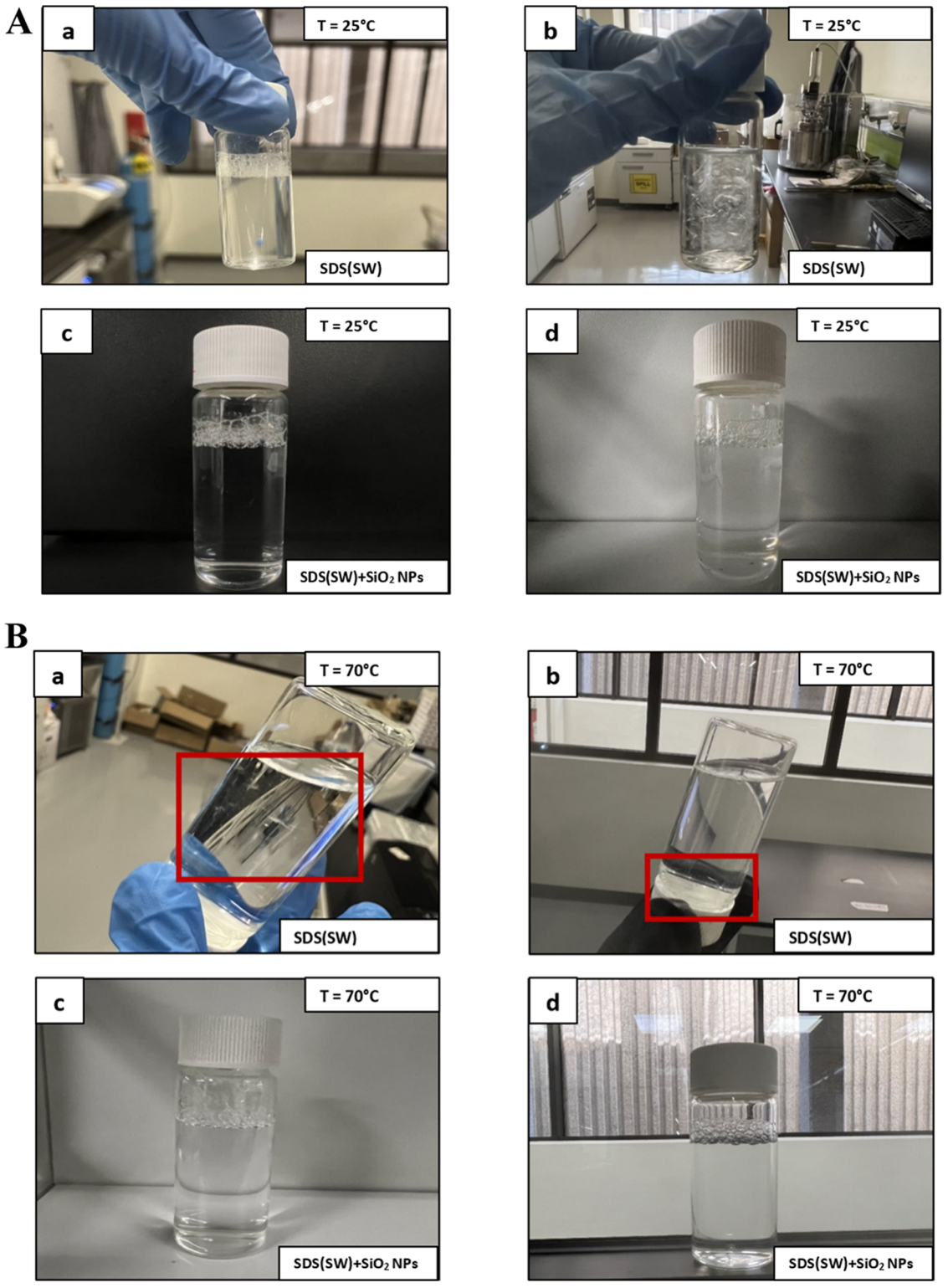

Figure 4. (A) (a) SDS on day one at 25 °C, (b) SDS on day seven at 25 °C, (c) SiO_2 nanofluid on day one at 25 °C, and (d) SiO_2 nanofluid on day seven at 25 °C. (B) (a) SDS on day one at 70 °C, (b) SDS on day seven at 70 °C, (c) SiO_2 nanofluid on day one at 70 °C, and (d) SiO_2 nanofluid on day seven at 70 °C.

DIW, and SiO_2 NPs in SW were considerably higher than those of SiO_2 nanofluid. This indicates that many particles began separating from the base fluid, leading to aggregation and precipitation. In the case of SDS in SW, this illustrates that the surfactant molecules started to crystallize and precipitate due to the strong ionic strength, which eventually resulted in reduced solubility and precipitation of SDS. These findings confirm the visual observations and, since this test was conducted at 70 °C, demonstrate that the precipitation of SDS is primarily due to ionic strength rather than the Krafft temperature.

The measurements were conducted over a single day for each sample, and fitting the separation rate over time enabled the

https://doi.org/10.1021/acsomega.4c08484
ACS Omega 2024, 9, 49804−49815

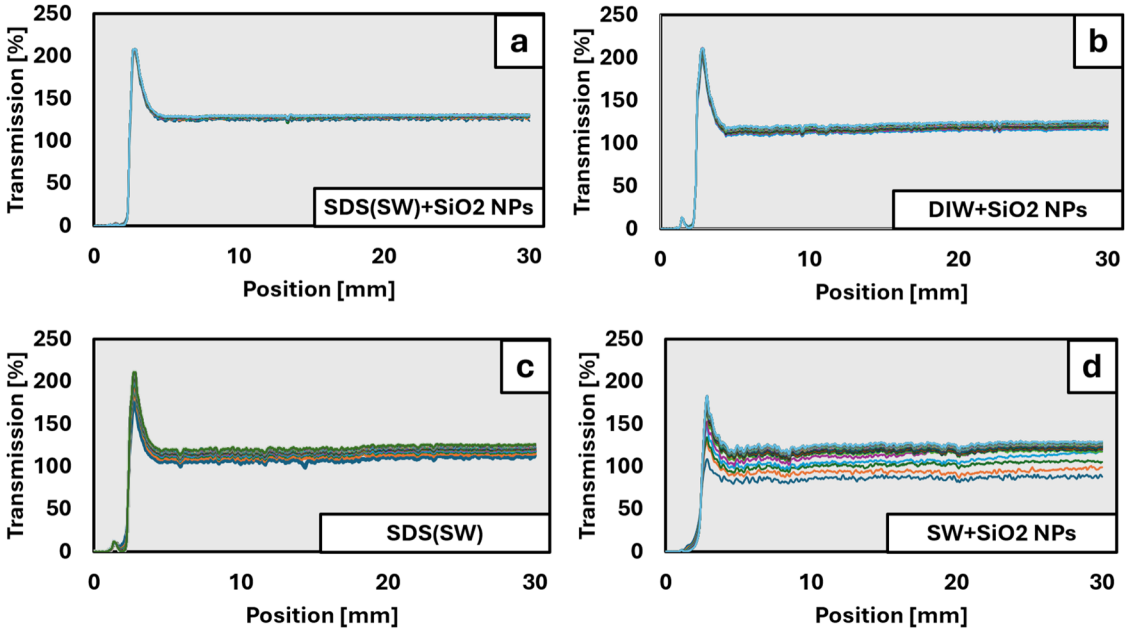

Figure 5. (a) Transmission profile of SDS(SW) + SiO_2 NPs after 1 day at 70 °C, (b) transmission profile of DIW + SiO_2 NPs after 1 day at 70 °C, (c) transmission profile of SDS(SW) after 1 day at 70 °C, and (d) transmission profile of SW + SiO_2 NPs after 1 day at 70 °C.

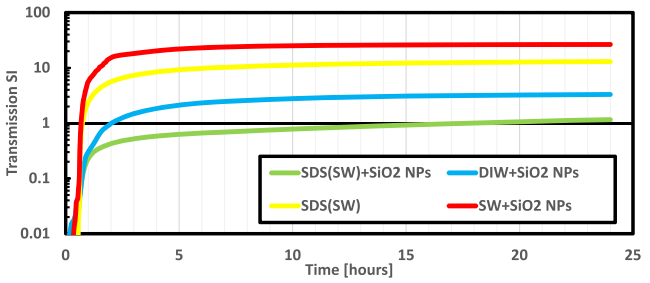

Figure 6. Transmission SI with time.

Table 3. Separation Rate Equations for Each Solution

sample	rate
SDS(SW) + SiO_2 NPs	$\frac{0.03556 + 0.0004543}{h}$
DIW + SiO_2 NPs	$\frac{0.1066 + 0.002336}{h}$
SDS(SW)	$\frac{0.291 + 0.006631}{h}$
SW + SiO_2 NPs	$\frac{0.6166 + 0.02233}{h}$

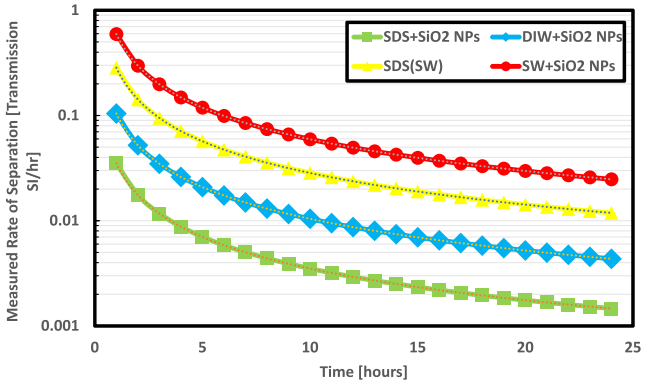

Figure 7. Rate of separation with time.

generation of predictive equations, as shown in Table 4, allowing us to forecast the separation rate over 7 days. The measured

Table 4. Prediction Equations Generated from Fitting the Data Using Power Trendline

sample	prediction eq
SDS(SW) + SiO_2 NPs	$\frac{0.0351}{t}$
DIW + SiO_2 NPs	$\frac{0.1043}{t}$
SDS(SW)	$\frac{0.2844}{t}$
SW + SiO_2 NPs	$\frac{0.5943}{t}$

separation profiles were then plotted alongside the predicted profiles to provide a more comprehensive understanding of the formulations' performance over a week, as illustrated in Figure 8. This approach offers valuable insights into the long-term stability and efficacy of the proposed formulations in maintaining nanoparticle dispersion and preventing aggregation and precipitation in high-salinity conditions.

The comparison between the measured and predicted profiles, as shown in Figure 8, confirms that our proposed

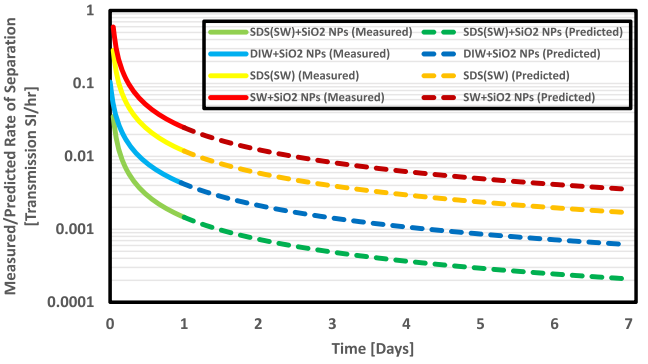

Figure 8. Predicted rate of separation with time for 7 days.

https://doi.org/10.1021/acsomega.4c08484
ACS Omega 2024, 9, 49804−49815

formulation exhibits the lowest separation rate at 70 °C. This signifies superior stability and dispersibility compared to other formulations, including SiO_2 in DIW, which has been extensively utilized in the literature and is presumed to be efficient. Notably, our formulation surpassed even this benchmark, highlighting its exceptional performance. In addition to the transmission and separation rate profiles, another valuable parameter is the separability number, which quantifies a formulation's tendency to separate.

It is worth mentioning that although SDS in SW initially showed more significant stability from visual observation on day seven compared to SiO_2 NPs in SW, the prediction curve still shows it as more stable than SiO_2 NPs in SW after a week. This is because the prediction is based on the data collected on day one. The precipitation phenomenon of SDS is complex and nonlinear, which likely explains why we observed higher precipitation on day seven despite initial turbidity measurements indicating a more stable profile than SiO_2 NPs in SW. The complexity and nonlinearity of SDS precipitation in SW initially contribute to more stable TSI profiles but not necessarily over extended periods.

Higher separability numbers indicate unstable and incompatible solutions, where separation occurs more rapidly than in stable solutions. As illustrated in Figure 9, the significant

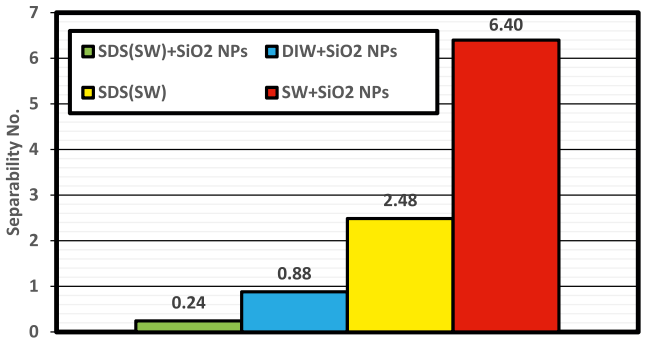

Figure 9. Separability number for the formulations utilized in this study.

difference in separability numbers underscores the superiority of our proposed formulation, which exhibits an exceptionally low value. In contrast, the other two solutions containing SiO_2 NPs and SDS in SW demonstrate relatively higher values. This disparity can be attributed to the enhanced dispersion of SiO_2 NPs facilitated by our novel formulation and the prevention of SDS precipitation. The combined advantages of our formulation in both aspects contribute to its remarkably low separability number, further validating its efficacy and potential in practical applications.

ζ-Potential. ZP measurements are vital to assess the solution's stability. ZP can be positive or negative and is key in determining the stability of nanofluids, colloidal systems, and surfactants.[56] A high absolute ZP value indicates a more stable and dispersed nanofluid. Conversely, a low absolute value of ZP signals a greater chance of the particles settling, aggregating, or precipitation molecules.[57]

Figure 10 shows the ZP profiles for the samples considered in this study for 7 days. Starting with the base case of DIW and SiO_2 NPs, we observe a relatively stable solution, as indicated by the absolute value of its ZP (ζ = 22.49 mV), attributed to the absence of salts, which did not cause any reductions in the overall charge due to ion exchanges when divalent are present. When different salts are added to the mix, the absolute value of

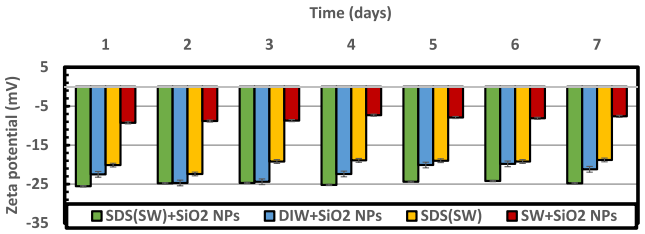

Figure 10. ζ-potential values for all formulations with time.

ZP decreases due to the suppression of the electric double layer around the SiO_2 NPs. This, coupled with a reduction in particle surface charge, causes the silica particles to clump together, as noted in previous studies.[58] This trend is evident in the second case, where SiO_2 NPs are introduced into SW, resulting in a significant decrease in the absolute value of ZP from (ζ = 22.49 mV to ζ = 9.27 mV).

The introduction of SDS to SW resulted in a higher absolute value of ZP (ζ = 20.12 mV) compared to the case of SW + SiO_2 NPs. However, as discussed earlier, SDS tends to precipitate over time due to its intolerance to high salinities. It should be noted that the absolute ZP value of SDS in DIW measured is (ζ = 64.95 mV) in this study, and similar values were obtained in the literature at varying SDS concentrations.[59−61] The significant difference between SDS value in DIW and SDS in SW highlights the impact of the complex salt system on the stability of the surfactant. Nonetheless, when SiO_2 NPs are added to SDS in SW, there is a subsequent increase in the absolute value of ZP (ζ = 25.55 mV). This is attributed to enhanced repulsions between the negatively charged SiO_2 NPs and SDS molecules with a negative headgroup. This confirms that our formulations are more electrostatically stable than SDS in SW. Therefore, this confirms that there are enhanced electrostatic repulsions that caused the overall mixture to be more stable and thus eliminated the possibility of precipitation based on visual observations, turbidity, and ZP measurements, as discussed previously. The magnitude of ZP predicts colloidal stability, with NPs having values >+25 or <−25 mV, usually indicating a high degree of stability.[62]

Hydrodynamic Diameter. SiO_2 NPs form fractal aggregates when the electrical double layer collapses at high salt concentrations, reducing stabilizing forces.[63] Accurate HDD measurements are crucial in nanotechnology, especially in cEOR, where SiO_2 NP aggregation poses a significant concern. As NP concentrations increase, collisions between particles may increase the potential for aggregations.[44] Thus, it is vital to consider HDD measurements to check the effectiveness of our optimal concentration and whether there is any aggregation. Furthermore, comparing our formulation with surfactant-free solutions is essential, especially considering the widespread use of SiO_2 in DIW, which has proven efficient in oil recovery.

Figure 11 presents the initial HDD values and standard deviations for the considered formulations. Notably, using SiO_2 NPs sized between 10−20 nm in the base fluid DIW resulted in a relatively small to medium particle aggregation (350 nm) with a uniform distribution. Conversely, when SW was the base fluid, a substantial aggregation occurred, measuring an HDD of 2570 nm; this reaffirms the previously mentioned complexity introduced by higher salinity base fluids, increasing the possibility of severe aggregations due to attractive forces between NPs and salt molecules.

https://doi.org/10.1021/acsomega.4c08484
ACS Omega 2024, 9, 49804−49815

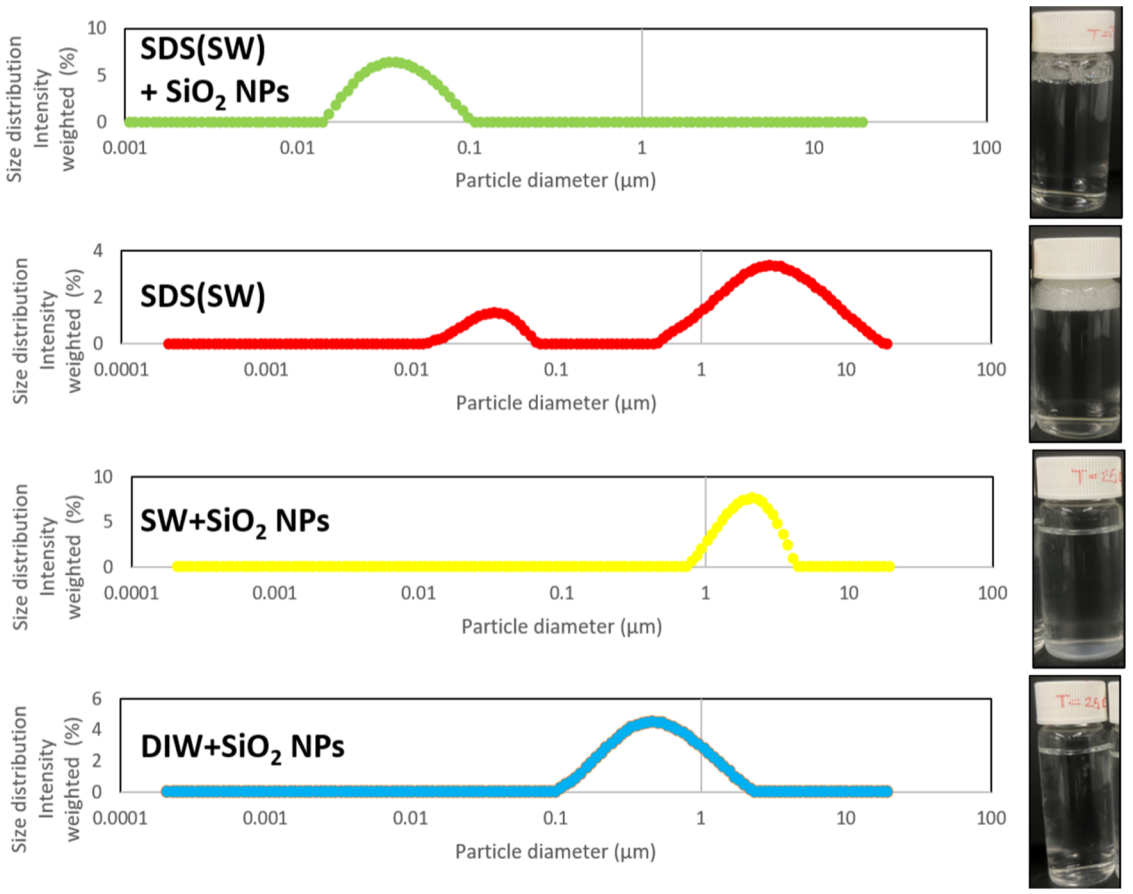

Figure 11. Initial HDD profiles prepared solutions.

A notable observation in the third case involving SDS revealed two distinct distributions. This phenomenon stemmed from SDS's intolerance to high salinity, resulting in precipitation. Two distributions are attributed to some SDS molecules precipitating while others remained dispersed. This unique occurrence was initially detected as the only solution to form precipitates, as indicated by the equipment. Moreover, a significant HDD of 1230 nm was observed, attributed to the aggregation of oppositely charged particles. Conversely, the final SiO_2 nanofluid sample exhibited a remarkably smaller HDD of 37 nm.

This underscores the accuracy of the selected optimal concentration in our study. Additionally, it highlights the efficacy of incorporating SDS to stabilize SiO_2 NPs in high-salinity solutions, showcasing a notable difference compared to SiO_2 NPs in SW. Intriguingly, the NPs also contributed to enhancing the aqueous stability of SDS, as evidenced by the absence of visual aggregations or precipitations, further confirmed by HDD measurements.

Figure 12 displays daily recordings of HDD values over 7 days. Predominantly, profiles exhibit minimal HDD variation, likely attributed to inherent equipment uncertainties. Notably, the SiO_2 nanofluid showcases remarkable stability throughout the seven-day duration, providing robust evidence that the proposed formulation effectively prevents aggregation within the specific time frame of this experiment.

Solution Stability Mechanism. As highlighted earlier, anionic surfactants, including SDS, exhibit intolerance to high salinities. Our investigations confirmed this characteristic, revealing a severe case of precipitation when SDS was formulated in a highly saline base fluid, as was shown in Figure 4A. However, the absence of precipitation is noteworthy when SDS is prepared using DIW as the base fluid as depicted in Figure 13.

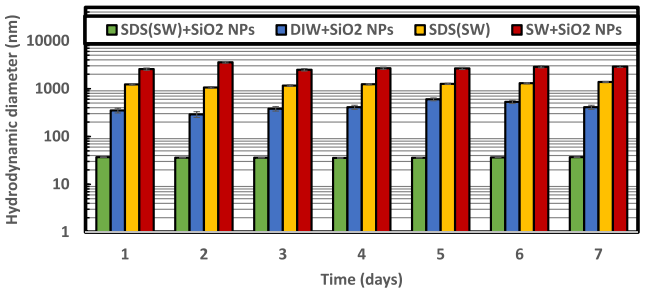

Figure 12. HDD values of prepared solutions for 7 days.

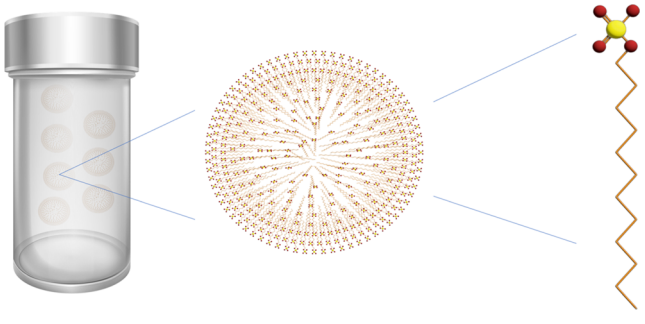

Figure 13. SDS in aqueous solutions that do not contain salt.

https://doi.org/10.1021/acsomega.4c08484
ACS Omega 2024, 9, 49804−49815

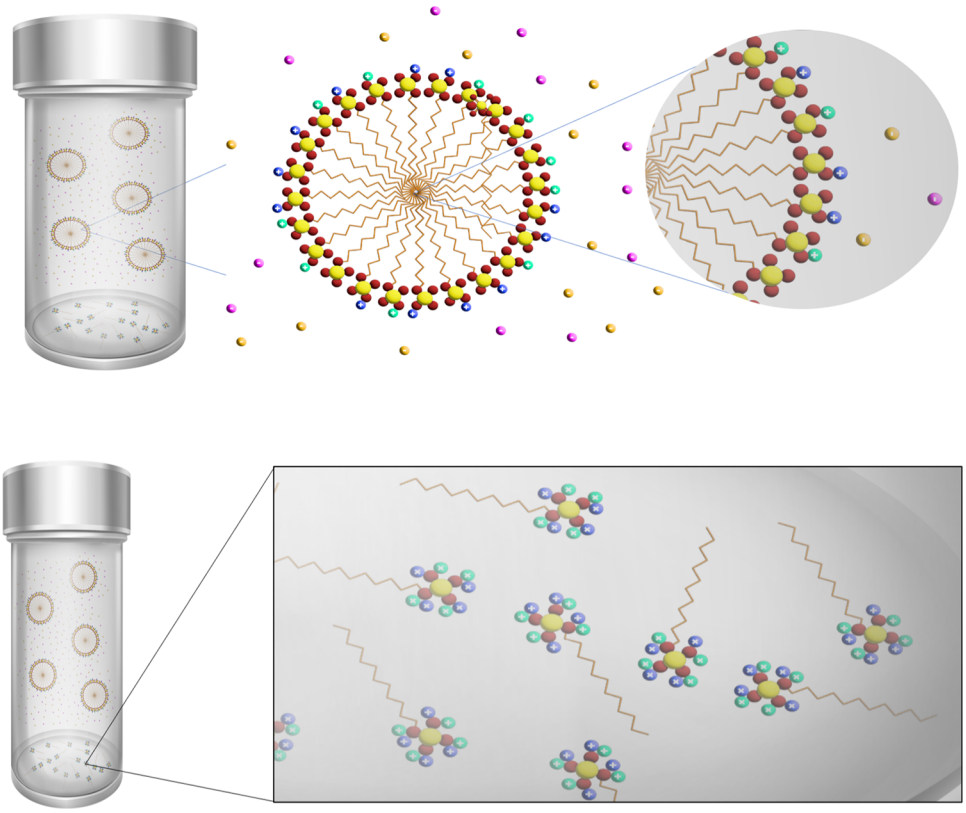

Figure 14. Precipitation of SDS due to its intolerance to high salinities.

Nevertheless, precipitation occurs when SDS is prepared with SW, unlike when SDS is mixed with DIW, as shown in Figure 13. Understanding the reasons behind SDS precipitation is crucial to appreciate how the proposed formulations address this issue. Introducing salts into the solution, particularly in complex systems with multiple and divalent ions, results in the presence of both positive and negative ions. The negative ions lack sufficient electrostatic repulsion to keep the molecules dissolved in SW, as evidenced by our ZP analysis in Figure 10. Consequently, aggregation occurs due to the positive charges from salts attracting the SDS negative head groups, as illustrated in Figure 14, forming solid precipitates. This does not occur in DIW due to the absence of divalent ions, which was confirmed through HDD analysis in Figure 12, where SDS gave an HDD of 1230 nm.

The results obtained in this study suggest that our proposed formulations provide steric stabilization by creating a physical barrier around SDS molecules, preventing aggregation and precipitation. Additionally, they enhance electrostatic repulsion between SDS molecules, further reducing the likelihood of aggregation. This improvement is demonstrated in Figure 4A when comparing SDS alone with SiO_2 nanofluid on a closer scale at a temperature of 25 °C.

To prevent this precipitation, either the salt concentration must be lowered, or an additive must be introduced to generate sufficient electrostatic repulsion, overcoming the attractions from the salt molecules and keeping SDS molecules in the solution. Traditionally, surfactants have been employed to stabilize SiO_2 NPs. However, this study takes a novel approach by using NPs to improve the aqueous stability of SDS and simultaneously utilizing SDS to stabilize SiO_2 NPs.

As evident in Figure 15, the surfactant head positions itself on the opposite side of the nanoparticle due to the repulsions

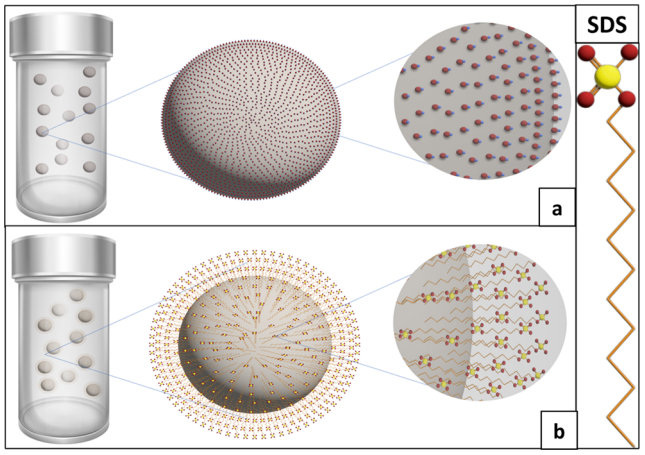

Figure 15. SDS negative head repulsions with SiO_2 NPs.

between the negatively charged SiO_2 NPs and the negative headgroup of SDS. These repulsions effectively maintain the dispersion of SDS molecules in SW, preventing aggregation. This was confirmed through an absolute ZP value of 25.55 mV, which was the highest value among all the formulations within this study, implying enhancement in electrostatic repulsions and, thus, better dispersion for NPs. It is crucial to highlight that this outcome was observed within what was identified as the optimal concentration of SiO_2 for this formulation, which was found to be (0.01 wt %), as mentioned earlier. This stabilization mechanism, achieved through enhanced electrostatic repulsions, may also extend to other anionic surfactants with similar molecular structures. The negatively charged head groups would similarly be repelled from the SiO_2 nanoparticle surfaces, positioning themselves on the opposite side of the NPs. This

https://doi.org/10.1021/acsomega.4c08484
ACS Omega 2024, 9, 49804−49815

separation between surfactant molecules—induced by the strong electrostatic repulsions—creates an effective spacing that reduces the likelihood of molecule clustering, thereby minimizing aggregation and maintaining stable dispersion even under high-salinity conditions.

CONCLUSIONS

This study introduced an innovative formulation combining silicon dioxide (SiO_2) nanoparticles with sodium dodecyl sulfate (SDS) to enhance the aqueous stability of anionic surfactants under extreme salinity and temperature conditions. By optimizing the SiO_2 nanoparticle concentration to 0.01 wt %, the formulation effectively mitigates SDS precipitation in brine with a high total dissolved salt concentration of 57,000 ppm. Remarkably, the solution demonstrates stability even after 7 days at temperatures up to 70 °C. This breakthrough offers substantial advancement for enhanced oil recovery (EOR) applications in the petroleum industry by addressing both performance and economic sustainability challenges.

Our findings reveal that the formulation exhibits robust stability across various reservoir conditions, with minimal changes in ζ-potential, hydrodynamic diameter, and turbidity over extended periods. This high degree of stability indicates the formulation's durability and scalability for industrial applications, marking a significant step forward for sustained EOR performance. Additionally, the dual stabilization mechanism—steric hindrance and electrostatic repulsion—achieved by incorporating SiO_2 nanoparticles is groundbreaking. It effectively prevents precipitation while enhancing surfactant dispersibility, which has been challenging to accomplish in high-salinity environments with previous methods.

This SiO_2 NP-based formulation also presents a cost-effective and environmentally sustainable alternative for the oil industry by utilizing seawater as the base fluid, thereby eliminating the need for expensive additives. This approach aligns with industry goals to reduce both operational costs and freshwater usage, underscoring its economic and ecological benefits. Furthermore, the study highlights areas for future research, including exploring the effects of high-pressure conditions, broader temperature ranges, and interactions with other surfactants commonly used in EOR. These studies could enhance the formulation's adaptability and effectiveness in a wider array of reservoir conditions.

In conclusion, this SiO_2 nanoparticle-based system represents a promising advancement for the oil industry. It offers a high-performance, sustainable EOR method that leverages readily available materials and seawater, positioning it as a cost-effective, environmentally responsible solution for improving oil recovery in challenging reservoir conditions.

AUTHOR INFORMATION

Corresponding Author

Muhammad Shahzad Kamal − *Department of Petroleum Engineering, King Fahd University of Petroleum & Minerals, Dhahran 34464, Saudi Arabia; Center for Integrative Petroleum Research, King Fahd University of Petroleum & Minerals, Dhahran 31261, Saudi Arabia;* orcid.org/0000-0003-2359-836X; Email: shahzadmalik@kfupm.edu.sa

Authors

Mohammed H. Alyousef − *Department of Petroleum Engineering, King Fahd University of Petroleum & Minerals, Dhahran 34464, Saudi Arabia*

Mobeen Murtaza − *Center for Integrative Petroleum Research, King Fahd University of Petroleum & Minerals, Dhahran 31261, Saudi Arabia;* orcid.org/0000-0003-4279-4665

Syed Muhammad Shakil Hussain − *Center for Integrative Petroleum Research, King Fahd University of Petroleum & Minerals, Dhahran 31261, Saudi Arabia;* orcid.org/0000-0002-6806-2326

Arshad Raza − *Department of Petroleum Engineering, King Fahd University of Petroleum & Minerals, Dhahran 34464, Saudi Arabia*

Shirish Patil − *Department of Petroleum Engineering, King Fahd University of Petroleum & Minerals, Dhahran 34464, Saudi Arabia;* orcid.org/0000-0002-0131-4912

Mohamed Mahmoud − *Department of Petroleum Engineering, King Fahd University of Petroleum & Minerals, Dhahran 34464, Saudi Arabia;* orcid.org/0000-0002-4395-9567

Complete contact information is available at: https://pubs.acs.org/10.1021/acsomega.4c08484

Notes

The authors declare no competing financial interest.

ACKNOWLEDGMENTS

The authors would like to acknowledge the invaluable support and encouragement provided by King Fahd University of Petroleum and Minerals (KFUPM) and the College of Petroleum Engineering and Geosciences (CPG).

REFERENCES

(1) Vaisman, L.; Wagner, H. D.; Marom, G. The role of surfactants in dispersion of carbon nanotubes. *Adv. Colloid Interface Sci.* **2006**, *128−130*, 37−46.

(2) Shaban, S. M.; Kang, J.; Kim, D.-H. Surfactants: Recent advances and their applications. *Compos. Commun.* **2020**, *22*, No. 100537.

(3) Massarweh, O.; Abushaikha, A. S. The use of surfactants in enhanced oil recovery: A review of recent advances. *Energy Rep.* **2020**, *6*, 3150−3178.

(4) Yang, W.; Lu, J.; Wei, B.; Yu, H.; Liang, T. Micromodel Studies of Surfactant Flooding for Enhanced Oil Recovery: A Review. *ACS Omega* **2021**, *6*, 6064−6069.

(5) Demirbas, A.; Alsulami, H. E.; Hassanein, W. S. Utilization of Surfactant Flooding Processes for Enhanced Oil Recovery (EOR). *Pet. Sci. Technol.* **2015**, *33*, 1331−1339.

(6) Keshtkar, S.; Sabeti, M.; Mohammadi, A. H. Numerical approach for enhanced oil recovery with surfactant flooding. *Petroleum* **2016**, *2*, 98−107.

(7) Al-Azani, K.; Abu-Khamsin, S.; Al-Abdrabalnabi, R.; Kamal, M. S.; Patil, S.; Zhou, X.; et al. Oil Recovery Performance by Surfactant Flooding: A Perspective on Multiscale Evaluation Methods. *Energy Fuels* **2022**, *36*, 13451−13478.

(8) Kamal, M. S.; Hussein, I. A.; Sultan, A. S. Review on Surfactant Flooding: Phase Behavior, Retention, IFT, and Field Applications. *Energy Fuels* **2017**, *31*, 7701−7720.

(9) Sircar, A.; Rayavarapu, K.; Bist, N.; Yadav, K.; Singh, S. Applications of nanoparticles in enhanced oil recovery. *Peres. Res.* **2022**, *7*, 77−90.

(10) Xiao, Z.; Dexin, L.; Lulu, L.; Yue, L.; Panhong, Y.; Jiaju, X.; et al. Synergistic effects of surfactants on depressurization and augmented injection in high salinity low-permeability reservoirs: Formula development and mechanism study. *Colloids Surf., A* **2021**, *628*, No. 127312.

(11) Belhaj, A. F.; Elraies, K. A.; Mahmood, S. M.; Zulkifli, N. N.; Akbari, S.; Hussien, O. S. The effect of surfactant concentration, salinity, temperature, and pH on surfactant adsorption for chemical enhanced oil recovery: a review. *J. Pet. Explor. Prod. Technol.* **2020**, *10*, 125−137.

(12) Sheng, J. J. Surfactant Flooding. In *Modern Chemical Enhanced Oil Recovery*; Elsevier, 2011; pp 239−335.
(13) Tavakkoli, O.; Kamyab, H.; Shariati, M.; Mustafa Mohamed, A.; Junin, R. Effect of nanoparticles on the performance of polymer/surfactant flooding for enhanced oil recovery: A review. *Fuel* **2022**, *312*, No. 122867.
(14) Kumar, R. S.; Al-Arbi Ganat, T.; Sharma, T. Performance evaluation of silica nanofluid for sand column transport with simultaneous wettability alteration: An approach to environmental issue. *J. Cleaner Prod.* **2021**, *303*, No. 127047.
(15) Hutin, A.; Lima, N.; Lopez, F.; Carvalho, M. Stability of Silica Nanofluids at High Salinity and High Temperature. *Powders* **2023**, *2*, 1−20.
(16) Bahari, N. M.; Che Mohamed Hussein, S. N.; Othman, N. H. Synthesis of $Al_2O_3 - SiO_2$ /water hybrid nanofluids and effects of surfactant toward dispersion and stability. *Part. Sci.Technology* **2021**, *39*, 844−858.
(17) Bai, Y.; Pu, C.; Li, X.; Huang, F.; Liu, S.; Liang, L.; Liu, J. Performance evaluation and mechanism study of a functionalized silica nanofluid for enhanced oil recovery in carbonate reservoirs. *Colloids Surf., A* **2022**, *652*, No. 129939.
(18) Roustaei, A.; Bagherzadeh, H. Experimental investigation of SiO2 nanoparticles on enhanced oil recovery of carbonate reservoirs. *J. Pet. Explor. Prod. Technol.* **2015**, *5*, 27−33.
(19) Raghav Chaturvedi, K.; Kumar, R.; Trivedi, J.; Sheng, J. J.; Sharma, T. Stable Silica Nanofluids of an Oilfield Polymer for Enhanced CO_2 Absorption for Oilfield Applications. *Energy Fuels* **2018**, *32*, 12730−12741.
(20) Singh, A.; Raghav Chaturvedi, K.; Sharma, T. An experimental evaluation of green surfactants to stabilize silica nanofluids in saline conditions and its application in CO_2 absorption. *Int. J. Chem. React. Eng.* **2024**, *22*, 1−9.
(21) Mohajeri, M.; Rasaei, M. R.; Hekmatzadeh, M. Experimental study on using SiO2 nanoparticles along with surfactant in an EOR process in micromodel. *Pet. Res.* **2019**, *4*, 59−70.
(22) Sharma, T.; Iglauer, S.; Sangwai, J. S. Silica Nanofluids in an Oilfield Polymer Polyacrylamide: Interfacial Properties, Wettability Alteration, and Applications for Chemical Enhanced Oil Recovery. *Ind. Eng. Chem. Res.* **2016**, *55*, 12387−12397.
(23) Xu, G.; Chang, J.; Wu, H.; Shao, W.; Li, G.; Hou, J.; et al. Enhanced oil recovery performance of surfactant-enhanced Janus SiO2 nanofluid for high temperature and salinity reservoir. *Colloids Surf., A* **2023**, *657*, No. 130545.
(24) Gomari, S. R.; Omar, Y. G. D.; Amrouche, F.; Islam, M.; Xu, D. New insights into application of nanoparticles for water-based enhanced oil recovery in carbonate reservoirs. *Colloids Surf., A* **2019**, *568*, 164−172.
(25) Chaturvedi, K. R.; Narukulla, R.; Amani, M.; Sharma, T. Experimental investigations to evaluate surfactant role on absorption capacity of nanofluid for CO2 utilization in sustainable crude mobilization. *Energy* **2021**, *225*, No. 120321.
(26) Mohajeri, M.; Hemmati, M.; Shekarabi, A. S. An experimental study on using a nanosurfactant in an EOR process of heavy oil in a fractured micromodel. *J. Pet. Sci. Eng.* **2015**, *126*, 162−173.
(27) Tian, S.; Gao, W.; Liu, Y.; Kang, W.; Yang, H. Effects of surface modification Nano-SiO2 and its combination with surfactant on interfacial tension and emulsion stability. *Colloids Surf., A* **2020**, *595*, No. 124682.
(28) Joshi, D.; Maurya, N. K.; Kumar, N.; Mandal, A. Experimental investigation of silica nanoparticle assisted Surfactant and polymer systems for enhanced oil recovery. *J. Pet Sci. Eng.* **2022**, *216*, No. 110791.
(29) Almitani, K. H.; Abu-Hamdeh, N. H.; Etedali, S.; Abdollahi, A.; Goldanlou, A. S.; Golmohammadzadeh, A. Effects of surfactant on thermal conductivity of aqueous silica nanofluids. *J. Mol. Liq.* **2021**, *327*, No. 114883.
(30) Han, S.; Gomez-Flores, A.; Choi, S.; Kim, H.; Lee, Y. A study of nanofluid stability in low−salinity water to enhance oil recovery: An extended physicochemical approach. *J. Pet. Sci. Eng.* **2022**, *215*, No. 110608.
(31) Zargartalebi, M.; Barati, N.; Kharrat, R. Influences of hydrophilic and hydrophobic silica nanoparticles on anionic surfactant properties: Interfacial and adsorption behaviors. *J. Pet. Sci. Eng.* **2014**, *119*, 36−43.
(32) Kumar, R. S.; Chaturvedi, K. R.; Iglauer, S.; Trivedi, J.; Sharma, T. Impact of anionic surfactant on stability, viscoelastic moduli, and oil recovery of silica nanofluid in saline environment. *J. Pet. Sci. Eng.* **2020**, *195*, No. 107634.
(33) Wang, W.; Gu, B.; Liang, L. Effect of Surfactants on the Formation, Morphology, and Surface Property of Synthesized SiO_2 Nanoparticles. *J. Dispersion Sci. Technol.* **2005**, *25*, 593−601.
(34) Hadia, N. J.; Ng, Y. H.; Stubbs, L. P.; Torsæter, O. High Salinity and High Temperature Stable Colloidal Silica Nanoparticles with Wettability Alteration Ability for EOR Applications. *Nanomaterials* **2021**, *11*, No. 707.
(35) Kumar, D.; Ganat, T.; Lashari, N.; Ayoub, M. A.; Kalam, S.; Chandio, T. A.; Negash, B. M. Experimental investigation of GO-HPAM and SiO2-HPAM composite for cEOR: Rheology, interfacial tension reduction, and wettability alteration. *Colloids Surf., A* **2022**, *637*, No. 128189.
(36) Jia, H.; Huang, W.; Han, Y.; Wang, Q.; Wang, S.; Dai, J.; et al. Systematic investigation on the interaction between SiO2 nanoparticles with different surface affinity and various surfactants. *J. Mol. Liq.* **2020**, *304*, No. 112777.
(37) Ramezani, M.; Abedini, R.; Lashkarbolooki, M. Experimental study about the effect of SiO2 nanoparticle in surfactant performance on IFT reduction and wettability alteration. *Chem. Eng. Res. Des.* **2023**, *192*, 350−361.
(38) Ahmed, M. E.; Sultan, A. S.; Al-Sofi, A.; Al-Hashim, H. S. Optimization of surfactant-polymer flooding for enhanced oil recovery. *J. Pet. Explor. Prod. Technol.* **2023**, *13*, 2109−2123.
(39) Almahfood, M.; Bai, B. The synergistic effects of nanoparticle-surfactant nanofluids in EOR applications. *J. Pet Sci. Eng.* **2018**, *171*, 196−210.
(40) Kazemzadeh, Y.; Sharifi, M.; Riazi, M.; Rezvani, H.; Tabaei, M. Potential effects of metal oxide/SiO2 nanocomposites in EOR processes at different pressures. *Colloids Surf., A* **2018**, *559*, 372−384.
(41) Rezvani, H.; Panahpoori, D.; Riazi, M.; Parsaei, R.; Tabaei, M.; Cortés, F. B. A novel foam formulation by Al2O3/SiO2 nanoparticles for EOR applications: A mechanistic study. *J. Mol. Liq.* **2020**, *304*, No. 112730.
(42) Harati, S.; Bayat, A. E.; Sarvestani, M. T. Assessing the effects of different gas types on stability of SiO2 nanoparticle foam for enhanced oil recovery purpose. *J. Mol. Liq.* **2020**, *313*, No. 113521.
(43) Hendraningrat, L.; Torsæter, O. Metal oxide-based nanoparticles: revealing their potential to enhance oil recovery in different wettability systems. *Appl. Nanosci.* **2015**, *5*, 181−199.
(44) Holthoff, H.; Egelhaaf, S. U.; Borkovec, M.; Schurtenberger, P.; Sticher, H. Coagulation Rate Measurements of Colloidal Particles by Simultaneous Static and Dynamic Light Scattering. *Langmuir* **1996**, *12*, 5541−5549.
(45) Keshavarzi, B.; Mahmoudvand, M.; Javadi, A.; Bahramian, A.; Miller, R.; Eckert, K. Salt Effects on Formation and Stability of Colloidal Gas Aphrons Produced by Anionic and Zwitterionic Surfactants in Xanthan Gum Solution. *Colloids Interfaces* **2020**, *4*, No. 9.
(46) Binks, B. P.; Shi, H. Aqueous Foams in the Presence of Surfactant Crystals. *Langmuir* **2020**, *36*, 991−1002.
(47) Li, P.; Wang, Z.; Ma, K.; Chen, Y.; Yan, Z.; Penfold, J.; et al. Multivalent electrolyte induced surface ordering and solution self-assembly in anionic surfactant mixtures: Sodium dodecyl sulfate and sodium diethylene glycol monododecyl sulfate. *J. Colloid Interface Sci.* **2020**, *565*, 567−581.
(48) Iyota, H.; Krastev, R. Miscibility of sodium chloride and sodium dodecyl sulfate in the adsorbed film and aggregate. *Colloid Polym. Sci.* **2009**, *287*, 425−433.
(49) Amani, P.; Firouzi, M. Effect of Divalent and Monovalent Salts on Interfacial Dilational Rheology of Sodium Dodecylbenzene Sulfonate Solutions. *Colloids Interfaces* **2022**, *6*, No. 41.

https://doi.org/10.1021/acsomega.4c08484
ACS Omega 2024, 9, 49804−49815

(50) Summerton, E.; Zimbitas, G.; Britton, M.; Bakalis, S. Crystallisation of sodium dodecyl sulfate and the corresponding effect of 1-dodecanol addition. *J. Cryst. Growth* **2016**, *455*, 111−116.
(51) Heakal, F. E. T.; Elkholy, A. E. Gemini surfactants as corrosion inhibitors for carbon steel. *J. Mol. Liq.* **2017**, *230*, 395−407.
(52) Vautier-Giongo, C.; Bales, B. L. Estimate of the Ionization Degree of Ionic Micelles Based on Krafft Temperature Measurements. *J. Phys. Chem. B* **2003**, *107*, 5398−5403.
(53) Nakayama, H.; Shinoda, K.; Hutchinson, E. The Effect of Added Alcohols on the Solubility and the Krafft Point of Sodium Dodecyl Sulfate. *J. Phys. Chem. A* **1966**, *70*, 3502−3504.
(54) Nakayama, H.; Shinoda, K. The Effect of Added Salts on the Solubilities and Krafft Points of Sodium Dodecyl Sulfate and Potassium Perfluoro-octanoate. *Bull. Chem. Soc. Jpn.* **1967**, *40*, 1797−1799.
(55) Li, S.; Ng, Y. H.; Lau, H. C.; Torsæter, O.; Stubbs, L. P. Experimental Investigation of Stability of Silica Nanoparticles at Reservoir Conditions for Enhanced Oil-Recovery Applications. *Nanomaterials* **2020**, *10*, No. 1522.
(56) Muneer, R.; Hashmet, M. R.; Pourafshary, P.; Shakeel, M. Unlocking the Power of Artificial Intelligence: Accurate ζ-potential Prediction Using Machine Learning. *Nanomaterials* **2023**, *13*, No. 1209.
(57) Pochapski, D. J.; dos Santos, C. C.; Leite, G. W.; Pulcinelli, S. H.; Santilli, C. V. ζ-potential and Colloidal Stability Predictions for Inorganic Nanoparticle Dispersions: Effects of Experimental Conditions and Electrokinetic Models on the Interpretation of Results. *Langmuir* **2021**, *37*, 13379−13389.
(58) Choi, W.; Mahajan, U.; Lee, S.-M.; Abiade, J.; Singh, R. K. Effect of Slurry Ionic Salts at Dielectric Silica CMP. *J. Electrochem. Soc.* **2004**, *151*, No. G185.
(59) Jia, W.; Ren, S.; Hu, B. Effect of Water Chemistry on ζ-potential of Air Bubbles. *Int. J. Electrochem. Sci.* **2013**, *8*, 5828−5837.
(60) White, B.; Banerjee, S.; O'Brien, S.; Turro, N. J.; Herman, I. P. Zeta-Potential Measurements of Surfactant-Wrapped Individual Single-Walled Carbon Nanotubes. *J. Phys. Chem. C* **2007**, *111*, 13684−13690.
(61) Khademi, M.; Wang, W.; Reitinger, W.; Barz, D. P. J. ζ-potential of Poly(methyl methacrylate) (PMMA) in Contact with Aqueous Electrolyte−Surfactant Solutions. *Langmuir* **2017**, *33*, 10473−10482.
(62) Shnoudeh, A. J.; Hamad, I.; Abdo, R. W.; Qadumii, L.; Jaber, A. Y.; Surchi, H. S.; Alkelany, S. Z. Synthesis, Characterization, and Applications of Metal Nanoparticles. *Biomater. Bionanotechnol.* **2019**, 527−612.
(63) Metin, C. O.; Bonnecaze, R. T.; Lake, L. W.; Miranda, C. R.; Nguyen, Q. P. Aggregation kinetics and shear rheology of aqueous silica suspensions. *Appl. Nanosci.* **2014**, *4*, 169−178.

https://doi.org/10.1021/acsomega.4c08484
ACS Omega 2024, 9, 49804−49815